Journal of
Nanoscience and Nanotechnology
Vol. 12, 3950–3953, 2012

RESEARCH ARTICLE

Experimental and Theoretical Study of the Optical and Electrical Properties of Nanostructured Indium Tin Oxide Fabricated by Oblique-Angle Deposition

Adam W. Sood[1,2,*], David J. Poxson[1], Frank W. Mont[1], Sameer Chhajed[1], Jaehee Cho[1], E. Fred Schubert[1], Roger E. Welser[2], Nibir K. Dhar[3], and Ashok K. Sood[2]

[1] Department of Electrical, Computer, and Systems Engineering, and Rensselaer Nanotechnology Center, Rensselaer Polytechnic Institute, Troy, NY 12180, USA
[2] Magnolia Optical Technologies, Inc., and Magnolia Solar, Inc., Woburn, MA 01801, USA
[3] Defense Advanced Research Projects Agency/Microsystems Technology Office (DARPA/MTO), Arlington, VA 22203, USA

Oblique-angle deposition of indium tin oxide (ITO) is used to fabricate optical thin-film coatings with a porous, columnar nanostructure. Indium tin oxide is a material that is widely used in industrial applications because it is both optically transparent and electrically conductive. The ITO coatings are fabricated, using electron-beam evaporation, with a range of deposition angles between 0° (normal incidence) and 80°. As the deposition angle increases, we find that the porosity of the ITO film increases and the refractive index decreases. We measure the resistivity of the ITO film at each deposition angle, and find that as the porosity increases, the resistivity increases superlinearly. A new theoretical model is presented to describe the relationship between the ITO film's resistivity and its porosity. The model takes into account the columnar structure of the film, and agrees very well with the experimental data.

Keywords: Oblique-Angle Deposition, Indium Tin Oxide, Optical Coating.

1. INTRODUCTION

Indium tin oxide (ITO) is a material that is widely used in electro-optical devices and nanostructure based solar cells requiring an optically transparent and electrically conducting layer. Belonging to the class of materials known as transparent conducting oxides, ITO is commonly used in the fabrication of LEDs, solar cells, LCD displays, touch-screen displays, etc.[1–5] For these applications, it would be useful to control the effective refractive index of a layer of nanostructured ITO while maintaining its high electrical conductivity.[6] The transmittance and reflectance of light at an interface between two layers are determined by the refractive indices of the layers, as described by the Fresnel equations. Therefore, the ability to control each layer's refractive index allows for the fabrication of optimal multilayer structures that maximize transmittance (i.e., anti-reflection coatings) or reflectance (i.e., distributed Bragg reflectors). In particular, low refractive index layers are essential in the design of optimal anti-reflection coatings and distributed Bragg reflectors.[7–10] Xi et al. have demonstrated the use of the oblique-angle deposition technique to fabricate optical coatings that have a low and controllable refractive index.[11] Xi et al. employed coatings made of SiO_2 and TiO_2, both of which are optically transparent yet electrically insulating materials, and demonstrated highly anti-reflecting structures using multiple layers of these coatings. More recently, Zhong et al.[12] and Leem et al.[13] studied ITO coatings fabricated by oblique-angle deposition. In the present work, we expand the work of these previous studies. We experimentally investigate the optical and electrical properties of nanostructured ITO coatings fabricated by the oblique-angle deposition technique, and we present a theoretical model.

Oblique-angle deposition is a technique, first demonstrated in 1886,[14] that uses a physical-vapor deposition technique, such as electron-beam evaporation, to deposit a material layer with a columnar nano-structure.[15–18] In oblique-angle deposition, the substrate is mounted at a certain non-normal angle θ inside the evaporation chamber, as

*Author to whom correspondence should be addressed.

illustrated in Figure 1. Initially, islands of evaporated material form on the substrate in random locations, as shown in Figure 2(a). Because the flux of evaporated material in a high-vacuum chamber flows from the source in only a straight line, and because the substrate is mounted at a non-normal angle to the direction of the vapor-flux, a shadow region forms behind each material island that the vapor-flux cannot reach. Thus, the vapor-flux does not coat the substrate uniformly, but instead nano-columns begin to preferentially grow from the islands, as illustrated in Figure 2(b). This nano-columnar layer can be described as having a certain volume porosity, defined as the volume of air within the layer divided by the total volume of the layer. At larger deposition angles (farther from normal), the nano-columns will be spaced farther apart, and thus the porosity will be greater. In addition, the refractive index of the layer will decrease as the porosity increases, as modeled by the linear-volume-approximation.[19]

In this study, the dependence of the porosity and the refractive index on the deposition angle is investigated for oblique-angle deposited ITO. The dependence of the electrical resistivity on the porosity of these ITO layers is also investigated. A theoretical model is presented to describe the relationship between the ITO film's resistivity and its porosity. The model takes into account the columnar structure of the film, and agrees very well with the experimental data.

2. EXPERIMENTAL DETAILS

We use 90% indium oxide/10% tin oxide (% by weight) for our ITO source material. Inside our electron-beam evaporation system, a sample mount has been fitted with a computer-controlled motor that can turn the sample to any deposition angle between 0 and 90°. During the deposition, the sample is held at a fixed deposition angle, and the deposition rate is held steady at 0.3 nm/s, as measured by a quartz crystal monitor inside the chamber. After the deposition, the samples are annealed, using a rapid thermal annealing (RTA) system, at 550 °C for 1 minute while flowing O_2. Variable-angle spectroscopic ellipsometry is used to determine the refractive index and the thickness of each ITO coating. The sheet resistance of each ITO coating is measured with a Lehighton contactless system.[20] Figure 3 is a photograph of select samples used in the experiment, illustrating the high optical quality of the ITO thin films.

3. RESULTS AND DISCUSSION

The experimentally-determined relationship between the ITO refractive index (measured by ellipsometry at

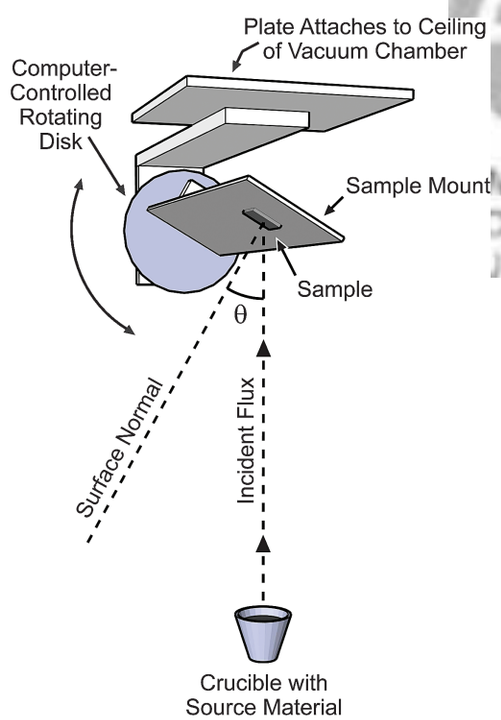

Fig. 1. Illustration of the experimental setup used in the oblique-angle deposition process. All objects in the illustration are inside the vacuum chamber of the e-beam evaporation system. The deposition angle θ is changed by rotating the mount with a computer-controlled motor.

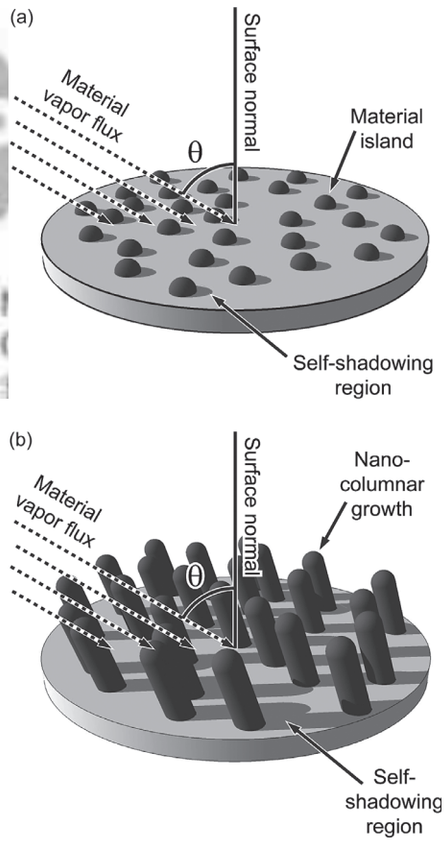

Fig. 2. Illustration of the growth of nano-columns on a substrate, during oblique-angle deposition. (a) Initially, material islands form in random locations on the substrate. (b) Due to the non-normal deposition angle θ, shadowing occurs behind the islands, causing columnar growth.

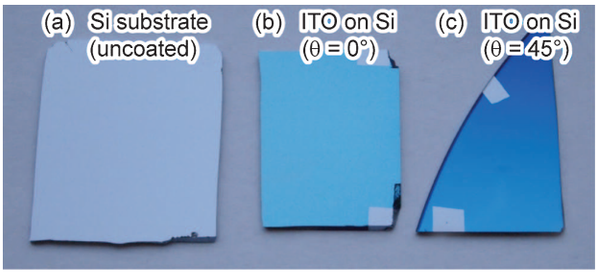

Fig. 3. Photograph of select samples used in the experiments: (a) uncoated Si substrate, and (b–c) Si substrates with ITO coatings, fabricated by oblique-angle deposition, with deposition angles $\theta = 0°$ (normal incidence) and $\theta = 45°$.

$\lambda = 462$ nm) and the deposition angle is shown in Figure 4. The calculated porosity is included in the same graph as a second ordinate. The relationship between the refractive index and the porosity of a nano-porous film is given by the linear volume approximation.[19] The experimental results in Figure 4 show that as the deposition angle increases, the refractive index decreases and the porosity increases. Poxson et al. developed a theoretical model for the relationship between the porosity and the deposition angle for films fabricated by the oblique-angle deposition method (this model is not specific to any one material).[21] This theoretical model fits very well with our experimental data (using the model parameter $c = 8.32$), with a correlation coefficient $R^2 = 0.99$. The theoretical curve is plotted in Figure 4, along with the experimental data. Our experimental data show that oblique-angle deposited ITO films can be used in optical applications which require a tailored refractive index in the range of 1.56–2.12 (the refractive index of the bulk ITO material is 2.12).

Figure 5 shows the experimentally-determined relationship between the resistivity and the porosity, indicated by the solid squares, for each ITO coating. The resistivity ρ of

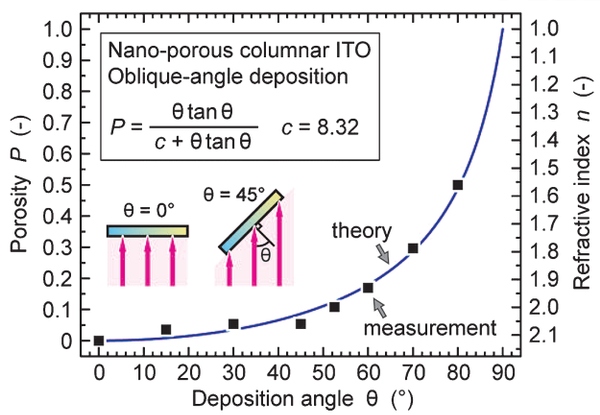

Fig. 4. Porosity calculated from measured refractive index (at $\lambda = 462$ nm), both plotted as a function of deposition angle, and theoretical curve from Poxson et al.,[21] using model parameter $c = 8.32$. An excellent fit between measurement and theory is obtained, with a correlation coefficient $R^2 = 0.99$.

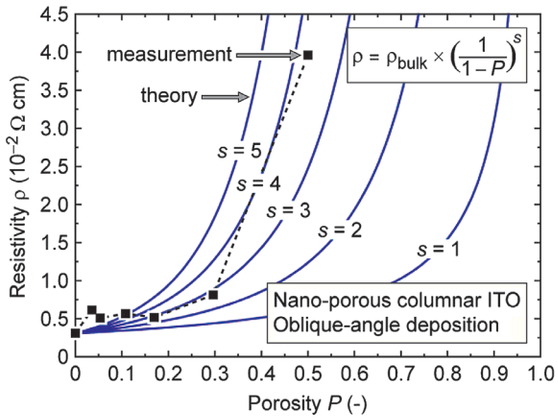

Fig. 5. ITO resistivity (calculated from measured sheet resistance) as a function of porosity (calculated from measured refractive index at $\lambda = 462$ nm), and a family of curves generated from the theoretical model described in the text, plotted with different values of parameter s. A very good fit between measurement and theory is obtained, with s ranging between 3 and 4.

each coating is calculated from the measured sheet resistance R_S and the measured thickness t_{layer} of each coating, using the standard formula: $\rho = R_S \times t_{layer}$. We present the relationship between the resistivity and the porosity, rather than the relationship between the resistivity and the deposition angle, because the porosity is the physical parameter of the film and is therefore more meaningful for the analysis. The experimental results in Figure 5 show that the resistivity is lowest in the bulk film (porosity = 0) and is highest in the most porous film (porosity = 0.5). As the porosity increases, the resistivity also increases. In the low-porosity region of this curve (porosity < 0.2), the slope of this curve is low. As the porosity increases, the slope increases. At porosity > 0.3, the slope becomes very steep. With regard to applications, this experimental curve shows that when the highest conductivity is needed for a layer, bulk ITO (porosity = 0) should be used. For applications that require good conductivity, ITO layers with porosity < 0.3 can be used. ITO layers with porosity > 0.3 are quite resistive and may not be useful as laterally conductive layers.

We have developed a theoretical model relating the resistivity ρ to the porosity P for these nano-porous columnar ITO films. As a starting point, we make the assumption that a film with porosity P and thickness t_{layer}, is equivalent (in terms of sheet resistance) to a bulk film (porosity = 0) with thickness $t_{equivalent} = (1 - P) \times t_{layer}$. For example, a film with a porosity of 30% and a thickness of 100 nm would be equivalent to a bulk film with a thickness of 70 nm. Under this assumption, it is simple to determine that the resistivity of the nano-porous film would be:

$$\rho = \rho_{bulk} \times \frac{1}{1-P} \quad (1)$$

where ρ_{bulk} is the resistivity of bulk ITO (porosity = 0). This assumption is not fully valid, however, because of the

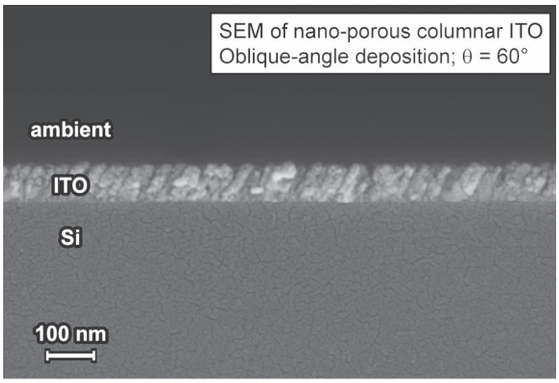

Fig. 6. Scanning electron micrograph (SEM) of a nano-porous columnar ITO coating, fabricated by oblique-angle deposition with a deposition angle of $\theta = 60°$, on a Si substrate.

columnar nanostructure of the film. Figure 6, for example, is an SEM image of an ITO film on a Si substrate that clearly shows the columnar nanostructure of the film. The near-vertical columns forming the film increase the resistivity in the lateral direction of the film, because it is difficult for the charge carriers to move from one column to the next. The resistivity of the real nano-columnar films rises faster with increasing porosity than Eq. (1) predicts. Therefore, we introduce a structural factor s to account for the increase in resistivity caused by the columnar morphology of the film. The revised equation is:

$$\rho = \rho_{\text{bulk}} \times \left(\frac{1}{1-P}\right)^{s} \quad (2)$$

Equation (2) is plotted in Figure 5, for different values of s (also note that the curve where $s = 1$ is equivalent to a plot of Eq. (1)). It is important to note that, for this entire family of curves (i.e., different values of s), $\rho = \rho_{\text{bulk}}$ when $P = 0$, and $\rho = \infty$ when $P = 1$. These two boundary conditions are required by the physical situation. The structural factor s does not have solely one physical meaning. It is an aggregate parameter that includes the resistivity-increasing effects caused by a number of physical properties of films fabricated by oblique-angle deposition. Two examples of these physical properties that necessitate the structural factor s are the near-vertical columnar morphology, and grain boundary potentials that increase with porosity (electrons have a higher probability of scattering at grain boundaries with higher potentials, thus increasing the material's resistivity).[12] Inspection of Figure 5 shows that our model fits very well with our experimental data, using a value for the structural factor s of between 3 and 4.

4. CONCLUSIONS

Our experimental results show that nanostructured ITO coatings fabricated by oblique-angle deposition can be useful in a variety of applications such as detectors, LEDs, and solar cells, which require an optically transparent and electrically conductive layer with a controllable refractive index. As the deposition angle increases, the porosity of the ITO increases and the refractive index decreases. As the films become more porous, the electrical resistivity increases superlinearly. We have developed a new theoretical model for the relationship between the ITO film's porosity and its resistivity. The model takes into account the nano-columnar structure of the film, and agrees very well with the experimental data.

Acknowledgments: The authors gratefully acknowledge support from the Department of Defense, National Science Foundation, and New York State Energy Research and Development Authority.

References and Notes

1. T. Margalith, O. Buchinsky, D. A. Cohen, A. C. Abare, M. Hansen, S. P. DenBaars, and L. A. Coldren, *Appl. Phys. Lett.* 74, 263930 (**2009**).
2. H. Kim, A. Pique, J. S. Horwitz, H. Mattoussi, H. Murata, Z. H. Kafafi, and D. B. Chrisey, *Appl. Phys. Lett.* 74, 233444 (**1999**).
3. Y. H. Tak, K. B. Kim, H. G. Park, K. H. Lee, and J. R. Lee, *Thin Solid Films* 411, 12 (**2002**).
4. J. Yang, A. Banerjee, and S. Guha, *Appl. Phys. Lett.* 70, 222975 (**1997**).
5. X. W. Sun, H. C. Huang, and H. S. Kwok, *Appl. Phys. Lett.* 68, 192663 (**1996**).
6. X. Yan, F. W. Mont, D. J. Poxson, M. F. Schubert, J. K. Kim, J. Cho, and E. F. Schubert, *Jpn. J. Appl. Phys.* 48, 120203 (**2009**).
7. A. Musset and A. Thelen, Progress In Optics VIII, North Holland Publishing Company, London (**1970**), pp. 203–240.
8. W. H. Southwell, *Opt. Lett.* 8, 584 (**1983**).
9. J. A. Dobrowolski, D. Poitras, P. Ma, H. Vakil, and M. Acree, *Appl. Opt.* 41, 3075 (**2002**).
10. D. Poitras and J. A. Dobrowolski, *Appl. Opt.* 43, 1286 (**2004**).
11. J. Q. Xi, M. F. Schubert, J. K. Kim, E. F. Schubert, M. Chen, S. Y. Lin, W. Liu, and J. A. Smart, *Nat. Photonics* 1, 176 (**2007**).
12. Y. Zhong, Y. C. Shin, C. M. Kim, B. G. Lee, E. H. Kim, Y. J. Park, K. M. A. Sobahan, C. K. Hwangbo, Y. P. Lee, and T. G. Kim, *J. Mater. Res.* 23, 2500 (**2008**).
13. J. W. Leem and J. S. Yu, *Opt. Express* 19, A258 (**2011**).
14. A. Kundt, *Ann. Phys. Chem.* 27, 59 (**1886**).
15. M. M. Hawkeye and M. J. Brett, *J. Vac. Sci. Technol. A* 25, 1317 (**2007**).
16. L. Abelmann and C. Lodder, *Thin Solid Films* 305, 1 (**1997**).
17. K. Robbie, J. C. Sit, and M. J. Brett, *J. Vac. Sci. Technol. B* 16, 1115 (**1998**).
18. K. Robbie and M. J. Brett, *J. Vac. Sci. Technol. A* 15, 1460 (**1997**).
19. W. H. Southwell, *Appl. Opt.* 24, 457 (**1985**).
20. G. L. Miller, D. A. H. Robinson, and J. D. Wiley, *Rev. Sci. Instrum.* 47, 799 (**1976**).
21. D. J. Poxson, F. W. Mont, M. F. Schubert, J. K. Kim, and E. F. Schubert, *Appl. Phys. Lett.* 93, 101914 (**2008**).

Received: 14 November 2011. Accepted: 6 February 2012.